

Electric monopole transitions in ^{40}Ca

M. Ulrickson* and N. Benczer-Koller

Department of Physics, Rutgers University, New Brunswick, New Jersey 08903[†]

Jack R. MacDonald[‡]

Bell Laboratories, Murray Hill, New Jersey 07974

J. W. Tape[§]

*Department of Physics, Rutgers University, New Brunswick, New Jersey 08903[†]
and Bell Laboratories, Murray Hill, New Jersey 07974*

(Received 24 September 1976)

The $E0$ pair decay branching ratio (Γ_π/Γ) for the 5.21-MeV 0^+ fifth excited state of ^{40}Ca was measured. The state was excited by inelastic proton scattering. The $e^- - e^+$ pairs were detected in two $\Delta E - E$ scintillation telescopes in coincidence with backscattered protons. A branching ratio limit of 1.4×10^{-3} was determined which corresponds to a monopole strength $\rho < 0.06$. This result is consistent with theoretical descriptions which contain multiparticle excitations and core deformations. In addition, the branching ratio $R((2_2^+ \rightarrow 0_2^+)/(2_2^+ \rightarrow 0_1^+)) = (2.1 \pm 0.1) \times 10^{-2}$ for the decay of 5.25-MeV 2^+ state was measured and corresponds to a $B(E2) = (3.5 \pm 0.6) e^2 \text{fm}^4$.

NUCLEAR REACTIONS $^{40}\text{Ca}(p, p')$, $E = 7-10$ MeV; ^{40}Ca , measured $E0$ branching ratios. Deduced $E0$ matrix elements. Natural targets.

I. INTRODUCTION

Electric monopole transitions proceed via two distinct modes, internal conversion and internal pair decay. The transition rate for both types is expressed¹ as a product of an electronic factor Ω , and the square of a nuclear "strength" parameter ρ which contains the nuclear structure information:

$$W = \Omega \rho^2.$$

The nuclear strength parameter is defined as

$$\rho = \frac{1}{R^2} \sum_p \int \psi_f r_p^2 \psi_i d\tau_{\text{nucl}},$$

where R is the nuclear radius, ψ_i and ψ_f are the initial and final nuclear wave functions, and the sum runs over protons only. Thus the $E0$ strength ρ is seen to be related to the overlap of the nuclear wave functions of excited and ground states and to the mean configuration radii.

Electric monopole transitions between 0^+ states have been studied extensively in light and medium weight nuclei. In particular, measurements of monopole transition rates in the calcium isotopes^{2,3} have strengthened models which describe the states involved as mixtures of shell-model and core-excited deformed states.⁴⁻⁶ For ^{40}Ca , ^{42}Ca , and ^{44}Ca , these interpretations predict significant proton-particle-hole components in the

wave functions of both ground and excited states. Such admixtures lead to large monopole strengths for the $0^+ \rightarrow 0^+$ transitions. In contrast, ^{48}Ca appears to be a "good" closed shell nucleus, and the monopole strength in this isotope is indeed very small.

The 0^+ first excited state of ^{40}Ca at 3.35 MeV is described as being mostly a 4p-4h core excited deformed state, and predictions^{4,6,7} of the monopole moment for the $E0$ transition to the ground state are in excellent agreement with the measured value obtained from the lifetime of the excited state⁸ and from electron scattering data.⁹ The second excited 0^+ state at 5.21 MeV is described as being mostly of 8p-8h nature.⁶ A measurement of the $E0$ branching ratio for the decay of this state to the ground state combined with the known lifetime¹⁰ might provide a good test of the model.

The $E0$ moments connecting 0^+ excited states to 0^+ ground states can be measured in a few selected cases by inelastic electron scattering^{9,11,12} or inelastic ^3He scattering.¹³ The majority of monopole transitions are best studied by direct measurement of lifetimes and branching ratios.^{14,2} Alburger and co-workers,¹⁴ in a series of measurements, have used an intermediate image magnetic spectrometer to study pair decay. A new technique which detects weak electron-positron pairs in competition with strong radiative cascades has been developed by Adloff *et al.*¹⁵ and is used in the present measurement.

II. EXPERIMENT

The energy levels, lifetimes, and known decay modes of the low-lying levels in ^{40}Ca are shown in Fig. 1. The observation of a monopole branch of order 10^{-3} from the 0^+ member of the triplet of states at 5.2-MeV demands a technique of high sensitivity. Adloff *et al.*¹⁵ have measured pair decay rates by directly detecting the electron and positron with high efficiency and good selectivity in a plastic scintillator pair spectrometer. Figure 2 shows a schematic diagram of the experimental arrangement. Two $\Delta E-E$ plastic scintillator telescopes operating in 2×2 coincidence were used for pair detection with excellent discrimination against photons and single electron events. States were excited by the $^{40}\text{Ca}(p, p')$ reaction on self-supported natural calcium targets, $280 \mu\text{g}/\text{cm}^2$ thick. The state of interest was singled out by requiring a further coincidence between the pair spectrometer quadruple coincidence system and a solid state annular detector selecting protons backscattered from the target. The target chamber was made as small as possible to increase the solid angle of the spectrometer and the amount of material

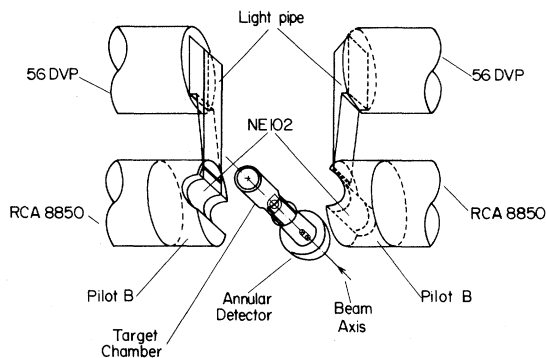


FIG. 2. Experimental arrangement of target chamber, quadruple scintillator pair spectrometer, and annular particle detector. The plastic scintillator telescopes are shown in a withdrawn position and the light-tight housing is not shown.

in the chamber was kept to an absolute minimum to reduce external pair production.

The thin plastic scintillators were constructed by bending 0.5-mm thick NE102 sheets at 100 C to form half-cylindrical detectors, 2.5 cm wide by 0.85 cm radius, which were in turn glued to Lucite light pipes with optical cement. These were mounted on Amperex 56DVP low noise photomultiplier tubes. The thick plastic detectors were constructed from 2.54-cm thick by 3.81-cm diam

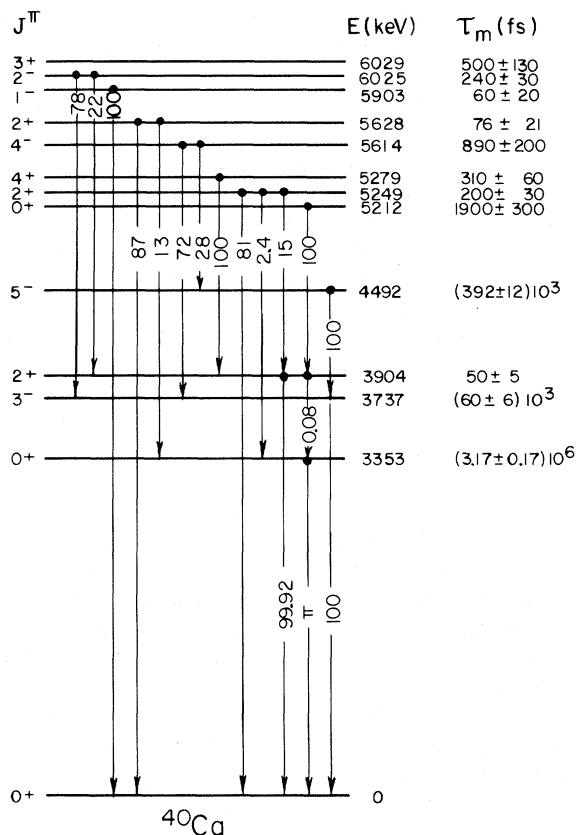


FIG. 1. Low-lying states of ^{40}Ca .

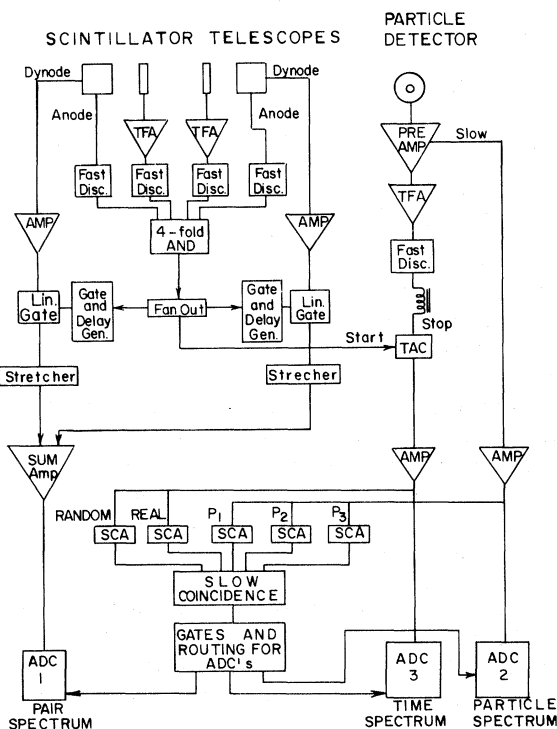


FIG. 3. Block diagram of the electronic system.

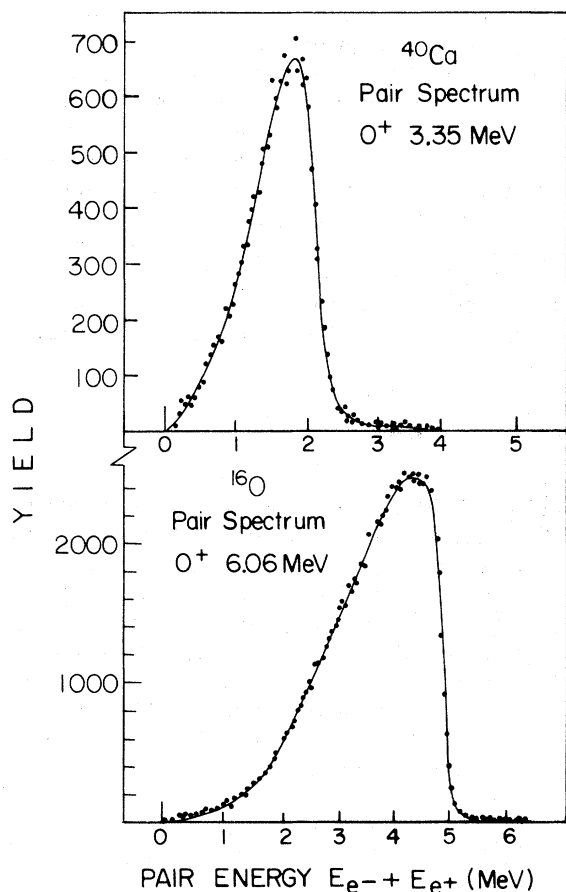


FIG. 4. Coincidence pair spectra from the decay of the ^{40}Ca , 3.35-MeV and ^{16}O , 6.06-MeV 0^+ states.

Pilot B scintillator and mounted on RCA 8870 photomultipliers. The thick plastic detectors had a half-cylindrical well machined into the front face to accommodate the thin detector. Light tightness between the two detectors was achieved by placing

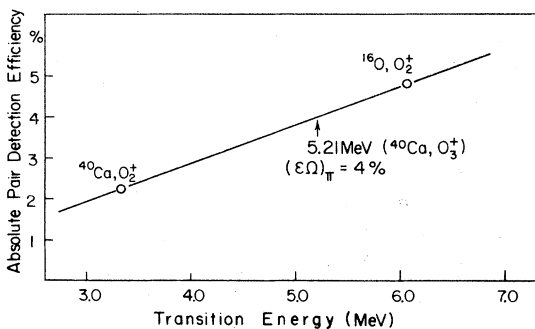


FIG. 5. Pair detection efficiency as a function of transition energy. The points labeled ^{16}O and ^{40}Ca are experimental points. The interpolated curve was calculated from the theoretical energy and angular distribution of the pairs and the geometry of the experiment.

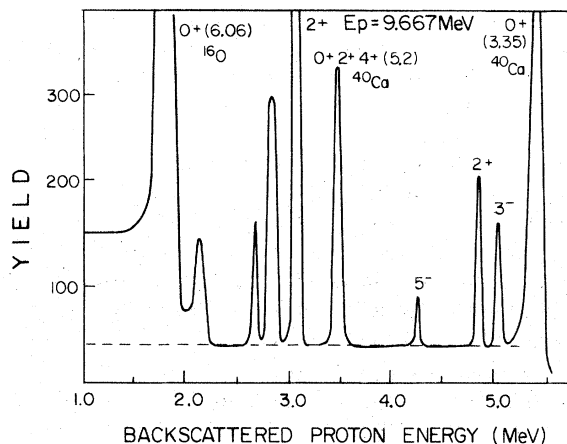


FIG. 6. Spectrum of protons observed in coincidence with electron-positron pairs.

a 0.005-mm thick aluminized Mylar foil between them.

The two telescopes fit around the target chamber, a stainless steel tube, 15.8 mm diam by 0.5 mm thick. Four 2.8-cm long openings were cut

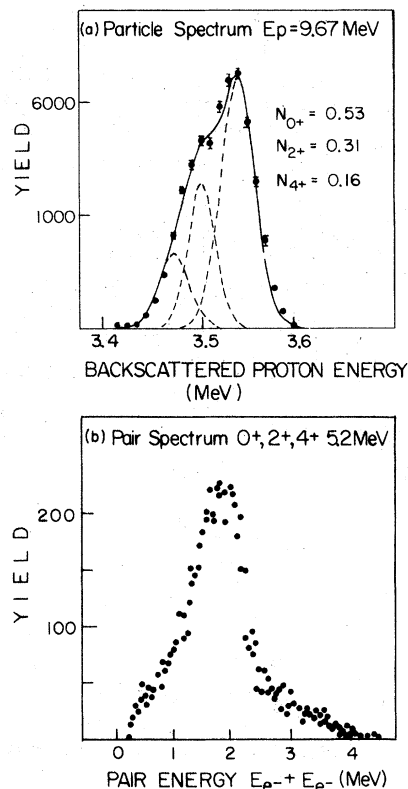


FIG. 7. (a) Coincidence proton spectrum from the 0^+ , 2^+ , 4^+ triplet of states in ^{40}Ca at 5.2 MeV. The dashed lines are Gaussian fits with relative intensities indicated. (b) Pair spectrum in coincidence with the proton groups of Fig. 7(a).

out of the chamber and were covered by 0.05-mm thick copper foil glued onto the rims of the chamber in order to maintain the beam line vacuum. A Mylar foil 38 mg/cm² thick was wrapped around the target chamber to prevent scattered protons from reaching the scintillator telescope. The target was centrally mounted such that each telescope subtended the angles: $\theta = 35^\circ$ – 145° and $\phi = 7^\circ$ – 86.5° , 93.5° – 173° , where θ and ϕ have their usual meaning. The annular particle detector was mounted a distance of 4.5 cm from the target.

Figure 3 shows a block diagram of the electronic system. The anode signals from the scintillator photomultipliers were appropriately amplified and sent to single level fast discriminators, thence to a 4-fold overlap coincidence circuit with 10-ns resolving time. The resulting quadruple coincidence output was used to start a time-to-amplitude converter (TAC) which was stopped by a particle timing signal. The amplified dynode signals from

the thick plastic detectors were summed after being gated by the quadruple coincidence requirement in order to obtain a total energy signal. Single channel analyzers were used to set windows on TAC real and random pulses, and on various particle groups of interest. Various combinations of these windows were fed into slow coincidence circuits whose outputs were used to gate and route the pair spectrometer total energy spectrum, the particle spectrum, and the TAC signals (Fig. 3). The resulting spectra were stored in various memory subgroups of a Xerox Data Systems $\Sigma 2$ computer.

III. DATA AND ANALYSIS

A. Efficiency measurement

Adloff *et al.*¹⁵ have shown that the efficiency of the detector telescope system is a strong function of the energy of the pair. Thus we measured the total absolute efficiency for pair detection at two energies which spanned the energy of interest and interpolated between the measured efficiencies using the method of Adloff *et al.*¹⁵ Figure 4 shows coincidence pair spectra from the 3.35-MeV (0^+) state of ^{40}Ca and the 6.06-MeV (0^+) state of ^{16}O . The spectra were taken with the same target

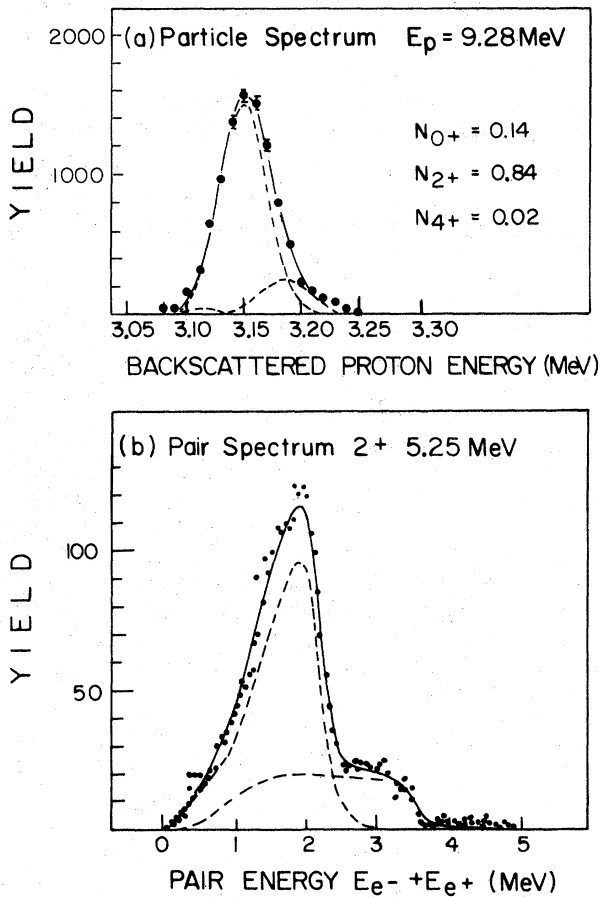


FIG. 8. (a) Coincidence particle spectrum in the region of the 5.2-MeV triplet at an incident proton energy of 9.28 MeV. (b) Pair spectrum from the decay of the 5.25-MeV (2^+) state.

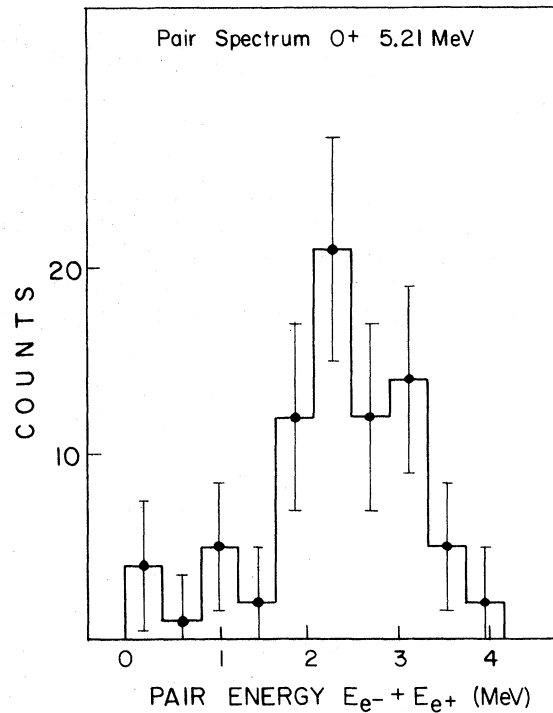


FIG. 9. Pair spectrum for the 5.21-MeV (0^+) state after subtracting from Fig. 7(b), the pair contributions from the unresolved 5.25-MeV (2^+) and 5.28-MeV (4^+) states.

TABLE I. Monopole transitions in the calcium isotopes.

	E (MeV)	J^π	τ (ps)	$\frac{0^+ \rightarrow 0^+}{0^+ \rightarrow 2^+}$	M (fm ²)	ρ (exp)	$\frac{M}{M^{\text{exp}}}$	ρ (theory)
⁴⁰ Ca	3.354	0 ₂ ⁺	3090 ± 220	1.0	2.6 ± 0.1	0.16 ± 0.01	0.12	(8p-8h) ^c
	5.212	0 ₃ ⁺	1.9 ± 0.3	<1.4 × 10 ⁻³	<1.01	<0.06	<0.02	0.15 3.1 2p + (4p-2h)
⁴² Ca	1.836	0 ₂ ⁺	480 ± 30	(0.88 ± 0.14) × 10 ⁻³	5.93 ± 0.52	0.34 ± 0.03	0.56	0.24 ^e
⁴⁴ Ca	1.883	0 ₂ ⁺	20 ± 6	(2.05 ± 0.17) × 10 ⁻²	5.38 ± 1.79	0.30 ± 0.10	0.43	4p + (6p-2h)
⁴⁸ Ca	4.284	0 ₂ ⁺	322 ± 16	0.225 ± 0.008	1.52 ± 0.07	0.084 ± 0.004	0.036	0.31 ^f

^aThe monopole single particle strength was defined by Wilkinson in Ref. 18.

^bSee Ref. 4.

^cSee Ref. 6.

^dSee Ref. 17.

^eSee Ref. 19.

^fSee Ref. 20.

(sufficient oxygen was present as a target impurity). Both of these states decay predominantly by electron-positron pairs. The absolute efficiencies of $(2.25 \pm 0.01) \times 10^{-2}$ and $(4.83 \pm 0.02) \times 10^{-2}$ for the 3.35- and 6.06-MeV transitions are shown on Fig. 5. The interpolated curve takes into account the energy and angular distributions of the electron-positron pairs,¹⁶ the geometry of the detector system and the low energy detection threshold due to absorbing material between target and detectors. An efficiency of $(4.0 \pm 0.1) \times 10^{-2}$ is deduced for a transition energy of 5.21 MeV.

B. Experimental results

Figure 6 shows a particle spectrum gated by events in the TAC real window (or equivalently by the quadruple coincidence gate from the pair spectrometer). In Fig. 7(a) the region around the peak of interest has been expanded to show the line shape observed at a proton bombarding energy of 9.667 MeV where the 5.21-MeV (0⁺) state is favorably excited. The contributions of the 0⁺, 2⁺, and 4⁺ states are indicated. Clearly the effect on the coincidence pair energy spectrum of the unresolved 2⁺ and 4⁺ members of the triplet as well as the background must be evaluated separately and taken into account. In addition, external pair formation from the 0⁺ decay γ - γ cascade will contribute pair events. Figure 7(b) shows the uncorrected e^-e^+ coincidence data obtained under the above experimental conditions, with random coincidences subtracted.

Three separate extraneous contributions to the pair spectrum can be identified from Figs. 6 and 7.

(1) The long tail in the particle spectrum extending to lower energies from the 3.35-MeV (0⁺) state is due to protons which have been degraded in energy by scattering either before or following excitation of the state. As this state decays 100% by pairs, even the relatively small number of counts appearing as a background in the window indicated in Fig. 7(a) contribute significantly to the coincident pair spectrum. Fortunately, the exact energy distribution of these pair events can be measured separately and subtracted (Fig. 4).

(2) All decay γ rays from the 5.2-MeV triplet are capable of contributing to the pair spectrum either through external pair production or from γ - γ cascades registered in the telescopes. These effects were estimated by accumulating pair spectra gated by protons exciting the 4.49-MeV state (γ - γ cascade and external pairs), the 3.90-MeV state (external pairs), and the 5.90-MeV state (external pairs). The detected rate of external pair formation varied from $(1.1 \pm 0.04) \times 10^{-4}$ per par-

ticle for the 5.90-MeV state to $(5.0 \pm 1.1) \times 10^{-5}$ per particle for the 3.90-MeV state. These results are consistent with the energy dependence of the pair production cross section.¹⁶ After accounting for the external pair formation rate in the decay of the 4.49-MeV state estimated from the external pair decay of the 3.90-MeV state, a residual γ - γ contribution of $(7.0 \pm 2.5) \times 10^{-5}$ per particle was deduced.

(3) As the 5.25-MeV (2^+) state is not resolved from the 5.21-MeV (0^+) state in the particle spectrum, its known decay to the 3.35-MeV (0^+) state will give rise to a real $E0$ contribution in the pair spectrum. This effect was investigated by accumulating the pair spectrum of Fig. 8(b) at a proton bombarding energy of 9.28-MeV where the 2^+ state is selectively excited [Fig. 8(a)]. Taking into account the effects of external pair production (deduced from the 5.90-MeV spectrum) and using a detection efficiency of 2.25×10^{-2} , a branching ratio of $(2.1 \pm 0.1) \times 10^{-2}$ was measured for the 5.25-MeV \rightarrow 3.35-MeV γ ray transition. These results yield a $B(E2) = 3.5 \pm 0.6 e^2 \text{ fm}^4$ for this transition.

Figure 9 shows the pair spectrum corresponding to the decay of the 0_3^+ (5.2 MeV) excited at a proton bombarding energy of 9.667 MeV. Contributions from the external pairs and γ - γ cascades from the 2^+ , 5.25-MeV and 4^+ , 5.28-MeV members of the poorly resolved triplet, as well as for the pairs contributed by the tail of the 0_1^+ (3.35 MeV) peak have been subtracted. The data of Fig. 9 must still be corrected for the effect of the γ - γ cascade from the 0_3^+ state itself. This correction was estimated from data obtained for the 5^- (4.49-MeV state) which decays by a similar cascade. After these contributions have been taken into account, there remain 34 ± 260 counts attributed to the $0_3^+ \rightarrow 0_1^+$ pair decay, corresponding to an upper limit on the branching ratio of 1.4×10^{-3} . Combining this limit on the branching ratio with the previously measured lifetime $\tau = 1.9 \pm 0.3$ ps,¹⁰ a limit on the monopole strength $\rho < 0.06$ is obtained. These results, together with the previous data on the decay of the 3.35-MeV 0_2^+ state, are shown in Table I. In addition, the monopole matrix elements as obtained from electron inelastic scattering are also shown. For comparison

the results from calculations based on different models are also given in columns 9, 10, and 11.

IV. DISCUSSION

The observed properties of the low-lying states of ^{40}Ca , ^{42}Ca , ^{44}Ca , and ^{48}Ca are well described by theoretical models which include low-lying particle-hole deformed states in addition to the usual shell-model states. Calculations of the ordering and spacing of the energy levels and of the transition rates between these states have been carried out by Gerace and Green⁴⁻⁶ on the basis of wave functions including up to 8p-8h configurations in the (fd) shell only. The experimental limit on the monopole strength ρ is consistent with the theoretical prediction $\rho = 0.08$ calculated using these wave functions. Similarly, excellent agreement between the monopole strength calculated in the coexistence model of Gerace and Green was found⁵ in the case of ^{42}Ca and ^{44}Ca . On the other hand, calculations based on the Federman and Pittel¹⁷ wave functions, which include only up to 4p-4h core excitation components and ignore deformations, while predicting with reasonable success the energy of the 0^+ and 2^+ states and the $B(E2)$ strength of many low-lying states, fail to predict the monopole decays of either the 3.35-MeV or the 5.21-MeV states of ^{40}Ca . Additional experimental evidence supporting an 8p-8h configuration for the 5.21-MeV state was obtained from heavy ion reaction studies. A band of states based on the 0_3^+ state was selectively populated in the transfer reaction $^{32}\text{S}(^{12}\text{C}, \alpha) ^{40}\text{Ca}$ which favors formation of 8p-8h states.²¹

The systematics of the measured ρ values for the Ca isotopes from ^{40}Ca to ^{48}Ca behave as expected. The ^{40}Ca , 3.35-MeV state, which is described in terms of multiple core-deformed states has a relatively large ρ value. As valence neutrons are added in going to ^{42}Ca and ^{44}Ca , the amount of core deformation increases and the values show a marked increase (Table I). In ^{48}Ca where the neutrons form a closed shell again, the amount of core deformation is substantially smaller (in fact, ^{48}Ca is described without invoking core deformation) and the ρ value shows a significant decrease.

*Present address: Plasma Physics Laboratory, Princeton University, P.O. Box 451, Princeton, New Jersey 08540.

†Work supported in part by the National Science Foundation.

‡Associate of the Faculty of Graduate Studies, Rutgers

University. Present address: Physics Department, University of Guelph, Guelph, Ontario, Canada.

§Present address: Los Alamos Scientific Laboratory, Group A-1, Los Alamos, New Mexico 87545.

¹E. L. Church and J. Weneser, Phys. Rev. **103**, 1035 (1965).

- ²N. Benczer-Koller, G. G. Seaman, M. C. Bertin, J. W. Tape, and Jack R. MacDonald, *Phys. Rev. C* 2, 1037 (1970).
- ³M. Ulrickson, W. Hartwig, N. Benczer-Koller, J. R. MacDonald, and J. W. Tape, *Phys. Rev. C* 13, 536 (1976).
- ⁴W. J. Gerace and A. M. Green, *Nucl. Phys.* 93, 110 (1967).
- ⁵W. J. Gerace and A. M. Green, *Nucl. Phys.* A113, 461 (1968).
- ⁶W. J. Gerace and A. M. Green, *Nucl. Phys.* A123, 241 (1969).
- ⁷G. F. Bertsch, *Nucl. Phys.* 89, 673 (1966).
- ⁸C. M. Bartle and P. A. Quin, *Nucl. Phys.* A216, 90 (1973).
- ⁹P. Strehl, *Z. Phys.* 234, 416 (1970).
- ¹⁰A. R. Poletti, A. D. W. Jones, J. A. Becker, and R. E. McDonald, *Phys. Rev.* 181, 1616 (1969).
- ¹¹P. Strehl and T. H. Schucan, *Phys. Lett.* 27B, 641 (1968).
- ¹²M. Stroezi, *Z. Phys.* 214, 357 (1968).
- ¹³H - P. Morsch, *Nucl. Phys.* A226, 506 (1974).
- ¹⁴E. K. Warburton and D. E. Alburger, *Phys. Rev. C* 10, 1570 (1974); J. W. Olness, W. R. Harris, A. Gallmann, F. Jundt, D. E. Alburger, and D. H. Wilkinson, *ibid.* 3, 2323 (1971), and references contained therein.
- ¹⁵J. C. Adloff, K. H. Souw, D. Disdier, F. Scheibling, P. Chevallier, and Y. Wolfson, *Phys. Rev. C* 10, 1819 (1974).
- ¹⁶R. H. Dalitz, *Proc. Roy. Soc.* A206, 521 (1951).
- ¹⁷P. Federman and S. Pettel, *Phys. Rev.* 186, 1106 (1969); *Nucl. Phys.* A139, 108 (1969).
- ¹⁸D. H. Wilkinson, *Nucl. Phys.* A133, 1 (1969).
- ¹⁹B. H. Flowers and L. D. Skouras, *Nucl. Phys.* A136, 353 (1969).
- ²⁰J. D. McCullen and D. J. Donahue, *Phys. Rev. C* 8, 1406 (1973).
- ²¹R. Middleton, J. D. Garrett, and H. T. Fortune, *Phys. Lett.* 39B, 339 (1972).